Electronic Supplementary Information

Ultrasmall Ru$_2$P nanoparticles on graphene: a highly efficient hydrogen evolution reaction electrocatalyst in both acidic and alkaline media

Tingting Liu, [a] Shuo Wang, [b] Qiuju Zhang, [b] Liang Chen,*[b] Weihua Hu,*[a] and Chang Ming Li [a]

[a] Institute for Clean Energy & Advanced Materials, Faculty of Materials & Energy

Southwest University, Chongqing 404100, China. Email: whhu@swu.edu.cn

[b] Ningbo Institute of Materials Technology and Engineering Chinese Academy of

Sciences, Ningbo 315201, China. Email: chenliang@nimte.ac.cn

Experimental Section

Materials

H_2SO_4 and KOH were purchased from Beijing Chemical Works Ltd. $RuCl_3 \cdot 3H_2O$, NaH_2PO_2, H_2O_2 (30 wt%), graphite and ethanol were purchased from Aladdin Reagents Ltd. $NaNO_3$, HCl, $KMnO_4$, Pt/C (20 wt%) and Nafion (5 wt%) were purchased from Sigma-Aldrich. All the reagents in the experiment were analytical grade and used as received. The deionized water (DI) used throughout all experiments was purified through a Millipore system.

Preparation of Graphite Oxide (GO)

GO was prepared according to reported method. In brief, graphite (2 g), $NaNO_3$ (1.2 g) and H_2SO_4 (76 mL) were stirred together in 0 ℃, followed by the slow addition of $KMnO_4$ (8.8 g) and stirred for about 12 h. Next, 72 mL DI was added and stirred for about 12 h in 50 ℃. Finally, 22 mL of H_2O_2 (30 wt%) was slowly added and stirred for about 3 h in 35 ℃. The solution was then filtered and washed with HCl several times. The product was then dispersed in water by mechanical agitation at 6000 rpm for 5 min. The final sediment was then washed with DI several times and followed by 6-h sonication to form the exfoliated GO.

Preparation of Ru_2P/RGO

The fabrication process for the Ru_2P/RGO was as follows. First, 20 mg $RuCl_3 \cdot 3H_2O$ was added to 30 mL of 1 mg mL^{-1} GO solution with stirring. Then, the solution was transferred to a 50 mL Teflon-sealed autoclave and heated at 160 ℃ for 12 h. The resulting black mixture was freeze-dried, and the black powder (Ru(III)/RGO) was collected. Second, the black powder and 2.0 g NaH_2PO_2 (weight ratio: 1:45) were grounded to form homogeneous powder. The powder was then annealed at 600 ℃ for 2 h under Ar atmosphere. After cooled to room temperature, the black products were collected, washed by centrifugation with deionized water several times to

remove the residue of reactants. Finally, the product was freeze-dried and denoted as Ru_2P/RGO-20. In addition, different amount of $RuCl_3 \cdot 3H_2O$ (10/40) also can be obtained Ru_2P/RGO (denoted as Ru_2P/RGO-10/Ru_2P/RGO-40). Ru_2P was also prepared according to the same method only using commercial RuO_2 instead of Ru(III)/RGO.

Preparation the working electrode

The catalyst powder (5.0 mg) was dispersed in 980 μL water/ethanol (v/v=1:1) mixed solvents along with 20 μL 5 wt% of Nafion solution, and the mixed solution was sonicated for 30 min. Then 14 μL of the catalyst ink was loaded on a glassy carbon electrode (GCE: diameter = 3 mm) at a catalyst loading of 1.0 mg cm^{-2}.

Preparation of Pt/C loaded electrode:

To prepare Pt/C electrode, 20 mg Pt/C (20 wt%) was dispersed in 1.0 mL 1:1 v water/ethanol solvent with 10 μL 5 wt% Nafion solution by 30-min sonication to form a catalyst ink. Then 50 μL of ink was loaded on a GCE with a catalyst loading of 1.0 mg cm^{-2} and therefore the Pt loading was 0.2 mg cm^{-2}.

Characterizations

Powder XRD data were collected on a Rigaku X-ray diffractometer equipped with a Cu Kα radiation source. XPS measurements were performed on an ESCALABMK II X-ray photoelectron spectrometer using Mg as the exciting source. SEM measurements were carried out on a XL30 ESEM FEG scanning electron microscope at an accelerating voltage of 20 kV. TEM measurements were performed on a HITACHI H-8100 electron microscopy (Hitachi, Tokyo, Japan) with an accelerating voltage of 200 kV. Raman spectra were obtained on J-Y T64000 Raman spectrometer with 514.5 nm wavelength incident laser light. ICP-AES analysis was performed on Optima 4300DV (Perkin Elmer Ltd., USA). Typically, 1.0 mg Ru_2P/RGO-20 was placed in a Teflon-lined autoclave, and 10 mL 65 wt% HNO_3 solution was then added.

The Teflon-lined autoclave was subsequently sealed and treated at 120 $^\circ$C for 48 h. After cooling to room temperature, the solution in the Teflon-lined autoclave was diluted with water to 100 mL in a volumetric flask. Using the ICP-AES elemental analyses and the concentration of Ru ions in the solution is 0.464 mg L^{-1}. The weight percent of Ru in the Ru$_2$P/RGO-20 is about (0.464 mg L^{-1}/10 mg L^{-1})*100% = 4.64%.

Electrochemical measurements

All electrochemical measurements were performed on a CHI-660-D electrochemical analyzer (CH Instruments, Inc., Shanghai) in a standard 3-electrode with 2-compartment cell. Prior to HER measurements, the electrolyte solution (0.5 M H$_2$SO$_4$ or 1.0 M KOH) was purged with N$_2$ for at least 5 min. The acidic (0.5 M H$_2$SO$_4$) electrochemical measurements were performed using a saturated calomel electrode (SCE) as the reference electrode. The alkaline (1.0 M KOH) electrochemical measurements were performed using a Hg/HgO as the reference electrode. A graphite plate was used as the counter electrode in all measurements. Polarization data were obtained at a scan rate of 5 mV s^{-1}. In all measurements, the reference electrode was calibrated with respect to reversible hydrogen electrode (RHE). All polarization curves were iR-corrected. Electrochemical impedance spectroscopy measurements were carried out in the frequency range of 100 kHz–0.1 Hz with AC amplitude of 10 mV at open circuit potential under H$_2$-saturated solution. iR correction was carried out according to the following equation: $E_{corr} = E_{mea} - iR$ (where E_{corr} is the iR-compensated potential, E_{mea} is the experimentally measured potential, and R is the solution resistance (R_s). The electrochemical impedance spectrum was fitted by using the ZView software and the parameters obtained are as follows.

Catalysts	R_s (Ω)	R_{ct} (Ω)	T ($\Omega^{-1}cm^{-2}s^n$)	n
Ru$_2$P/RGO-20	13.7	55.5	3.88×10^{-3}	0.59
Ru$_2$P	5.1	1422	4.56×10^{-5}	0.83

The Faradic efficiency (FE) is defined as the ratio of the amount of experimentally determined hydrogen to that of the theoretically expected hydrogen. The hydrogen gas was collected by the water drainage method. A constant potential was applied on the electrode and the volume of evolved gases was recorded synchronously. Then the moles of H_2 were calculated based on the gas laws. The theoretically expected amount of H_2 was then calculated by applying the Faraday law, which states that the passage of 96500 C causes 1 equivalent of reaction.

Theoretical calculation

Computation details: Spin-polarized density functional theory calculations were performed using the Vienna ab initio simulation package (VASP).[1-3] We used the PBE functional for the exchange-correlation energy[4] and projector augmented wave (PAW) potentials.[5,6] The kinetic energy cutoff was set to 450 eV. The ionic relaxation was performed until the force on each atom is less than 0.02 eV/Å. The k-points meshes were 6×4×2 with Monkhorst-Pack method.[7] The simulations were performed based on a $Ru_2P(112)$ slab model and Ru_2P/RGO-20 interface with one Ru_2P unit on the graphene substrate. To minimize the undesired interactions between images, a vacuum of at least 10 Å was considered along the z axis.[8] The free energy change for H* adsorption on catalyst surfaces (ΔG_{H^*}) was calculated as follows, which is proposed by Norskov and coworkers:[9]

$$\Delta G_{H^*} = E_{total} - E_{sur} - E_H{}^2/2 + \Delta E_{ZPE} - T\Delta S$$

where E_{total} is the total energy for the adsorption state, E_{sur} is the energy of pure surface, $E_H{}^2$ is the energy of H_2 in gas phase, ΔE_{ZPE} is the zero-point energy change and ΔS is the entropy change.

References

[1] G. Kresse, J. Furthmuller, *Comp. Mater. Sci.* **1996**, *6*, 15–50.
[2] G. Kresse, J. Furthmuller, *Phys. Rev. B* **1996**, *54*, 11169–11186.

[3] G. Kresse, J. Hafner, *Phys. Rev. B* **1994**, *49*, 14251–14269.

[4] J. P. Perdew, K. Burke, M. Ernzerhof, *Phys. Rev. Lett.* **1997**, *78*, 1396–1396.

[5] G. Kresse, D. Joubert, *Phys. Rev. B* **1999**, *59*, 1758–1775.

[6] P. E. Blochl, *Phys. Rev. B* **1994**, *50*, 17953–17979.

[7] H. J. Monkhorst, J. D. Pack, *Phys. Rev. B* **1976**, *13*, 5188–5192.

[8] G. Henkelman, B. P. Uberuaga, P. Jonsson, *J. Chem. Phys.* **2000**, *113*, 9901–9904.

[9] J. K. Noskov, T. Bligaard, A. Logadottir, J. R. Kitchin, J. G. Chen, S. Pandelov, U. Stimming, *J. Electrochem. Soc.* **2005**, *152*, J23–J26.
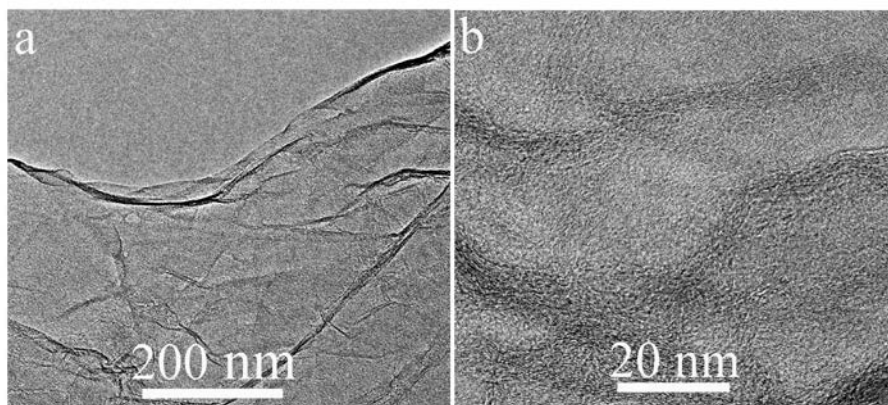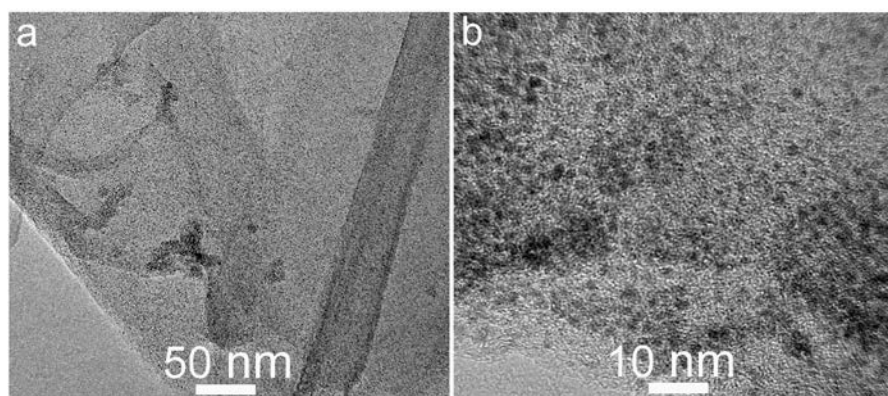
Fig. S1 TEM images of as-prepared GO.

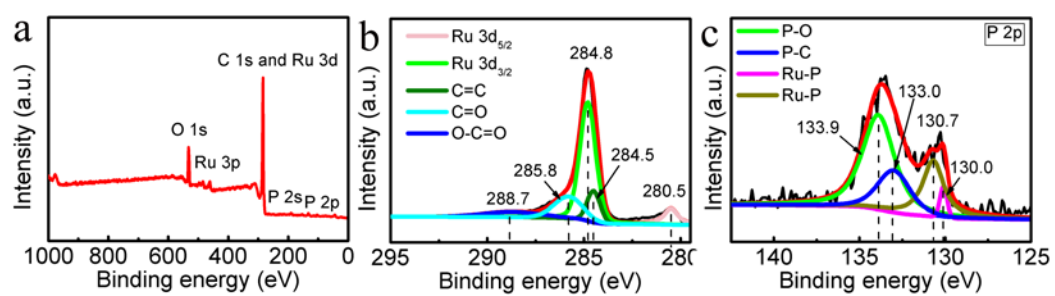**Fig. S2** TEM images of Ru (III) ultrasmall nanoparticles on RGO.

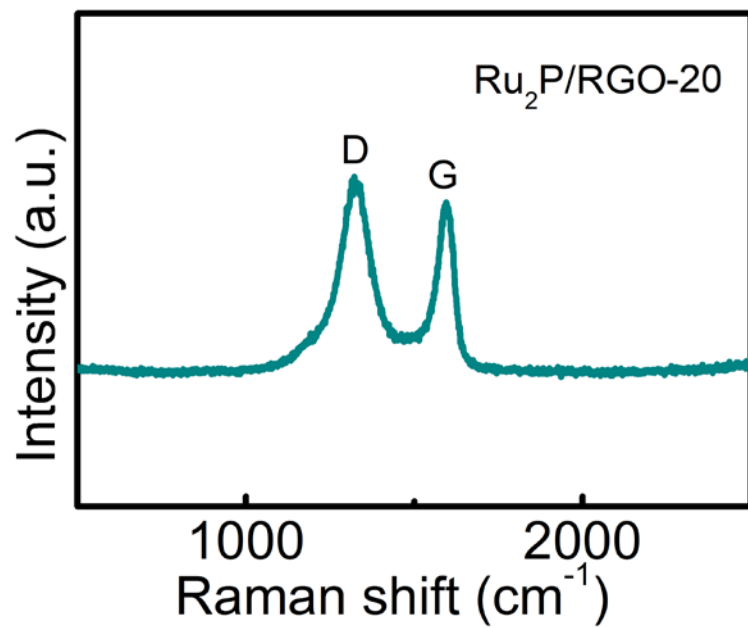**Fig. S3** XPS spectra for Ru$_2$P/RGO-20.

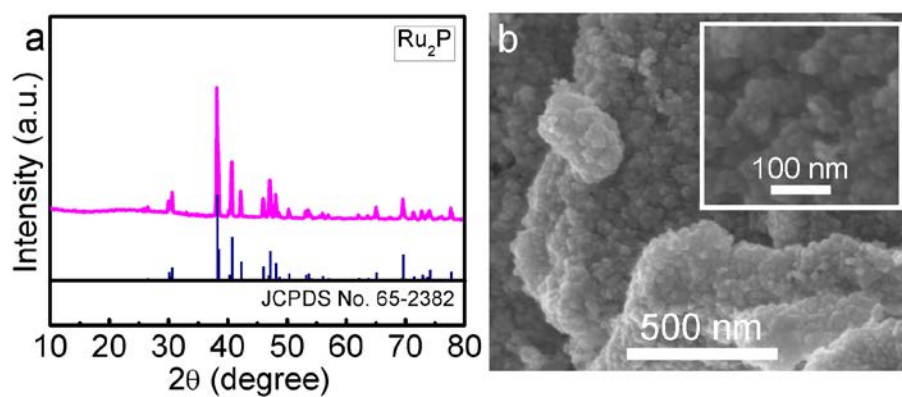**Fig. S4** Raman spectra of Ru$_2$P/RGO-20.

Fig. S5 (a) XRD pattern of Ru$_2$P. (b) Low- and high-magnification SEM images of Ru$_2$P.
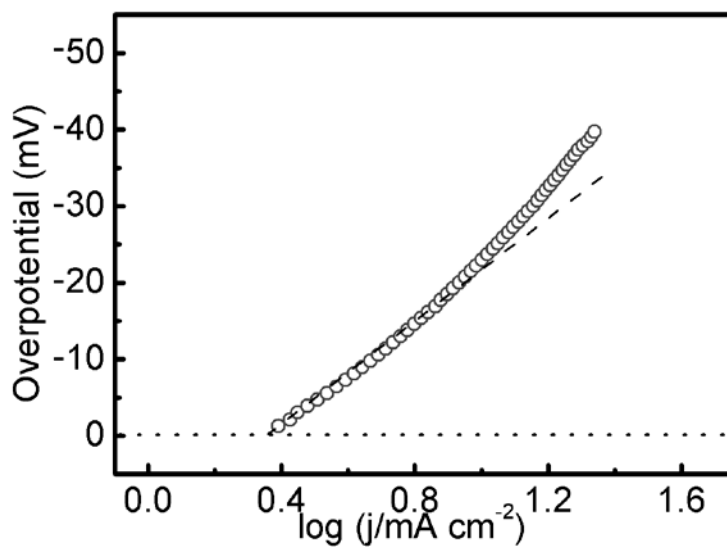
Fig. S6 Calculation of exchange current density of Ru$_2$P/RGO-20 by applying extrapolation method to the Tafel plot.
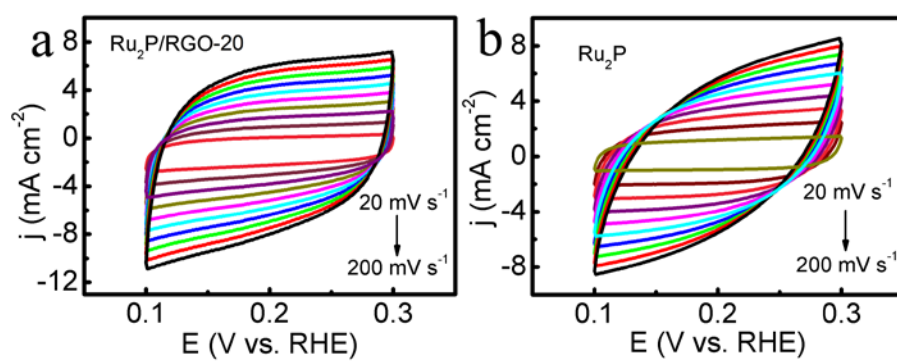

Fig. S7 CVs for (a) Ru$_2$P/RGO-20 and (d) Ru$_2$P.
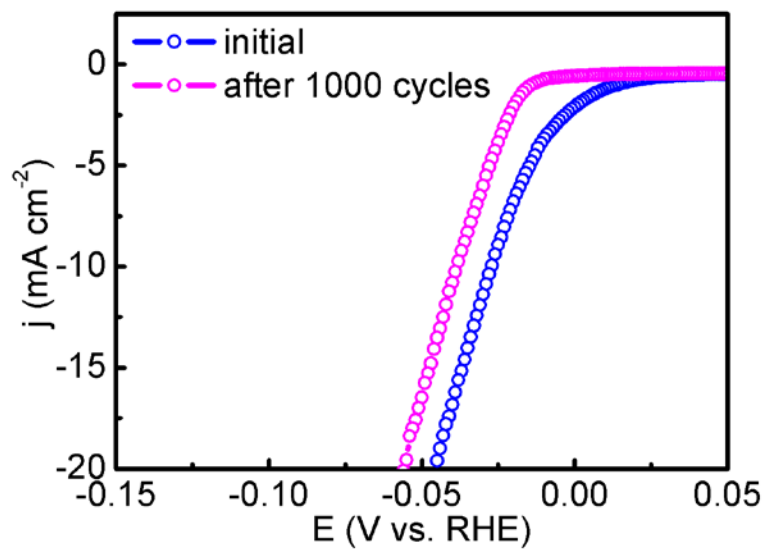
Fig. S8 HER polarization curves were recorded before and after 1000 CV cycles for Pt/C in 0.5 M H_2SO_4 solution.
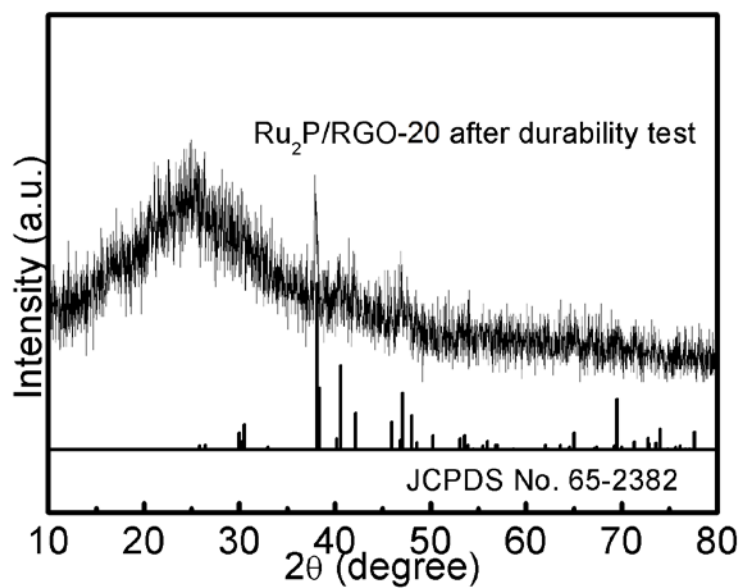
Fig. S9 XRD pattern of Ru_2P/RGO-20 after durability test.
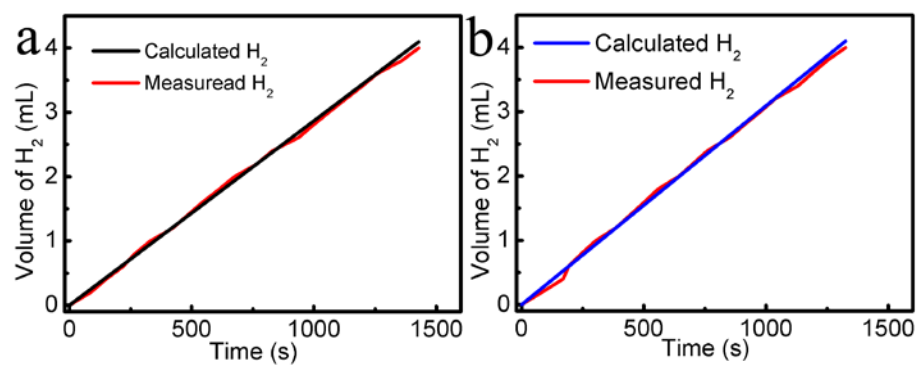
Fig. S10 Hydrogen production efficiencies for HER under potentiostatic electrolysis with the Ru$_2$P/RGO-20 under (a) acidic (at constant potential of -43 mV) and (b) alkaline media (at constant potential of -35 mV). The calculated H$_2$ lines represent the theoretical H$_2$ amount of assuming a quantitative Faradaic yield. The measured H$_2$ lines represent the experimentally measured H$_2$ (red line).

Table S1. Comparison of HER performance in acid/alkaline media for Ru_2P/RGO-20 with other HER electrocatalysts.

Catalysts	Electrolytes/(pH)	Overpotential@j (mV@mA cm^{-2})	Tafel slope (mV dec^{-1})	Catalyst loading (mg cm^{-2})	Ref.
Ru_2P/RGO-20	0.5 M H_2SO_4	-22@10	-29	1.0	This work
	1.0 M KOH	-13@10	-40		
CoP/CC	0.5 M H_2SO_4	-67@10	-51	0.92	[1]
	1.0 M KOH	-209@10	-129		
CoP@BCN	0.5 M H_2SO_4	-87@10	-46	0.4	[2]
	1.0 M KOH	-215@10	-52		
WP_2 SMPs	0.5 M H_2SO_4	-161@10	-57	0.5	[3]
	1.0 M KOH	-153@10	-60		
WP_2 NPs/W	0.5 M H_2SO_4	-143@10	-66	0.2	[4]
	1.0 M KOH	-214@10	-92		
WP NPs@NC	0.5 M H_2SO_4	-102@10	-58	2.0	[5]
	1.0 M KOH	-150@10			
MoP_2 NS/CC	0.5 M H_2SO_4	-58@10	-63.6	0.8	[6]
	1.0 M KOH	-85@10	-70.0		
MoP NA/CC	0.5 M H_2SO_4	-124@10	-58	2.5	[7]
	1.0 M KOH	-80@10	-83		
$NiCo_2P_x$/CF	0.5 M H_2SO_4	-104@10	-59.6	5.9	[8]
	1.0 M KOH	-58@10	-34.3		
np-$(Co_{052}Fe_{0.48})_2P$	0.5 M H_2SO_4	-64@10	-45	2.5	[9]
	1.0 M KOH	-79@10	-40		
Ni_2P/Ti	0.5 M H_2SO_4	-130@20	-46	1.0	[10]
Ni_2P	0.5 M H_2SO_4	-140@20	-66	0.38	[11]
	1.0 M KOH	-250@20	-102		
NiP_2 NS/CC	0.5 M H_2SO_4	-75@10	-51	4.3	[12]

	1.0 M KOH	-102@10	-65		
CoP/CNT	0.5 M H$_2$SO$_4$	-122@10	-54	0.285	[13]
CoP/Ti	0.5 M H$_2$SO$_4$	-85@20	-50	2.0	[14]
Co-P/Cu foil	1.0 M NaOH	-94@10	-42	-	[15]
FeP	0.5 M H$_2$SO$_4$	-50@10	-37	1.0	[16]
MoP	0.5 M H$_2$SO$_4$	-180@30	-54	0.86	[17]
Mo$_2$C@NC	0.5 M H$_2$SO$_4$	-124@10	-	0.28	[18]
	1.0 M KOH	-60@10	-		
15-h-CoS$_2$	0.5 M H$_2$SO$_4$	-200@12.37	-72	-	[19]
	1.0 M KOH	-244@10	-133		
Co-NCNT/CC	0.5 M H$_2$SO$_4$	-78@10	-74	3.4	[20]
	1.0 M KOH	-180@10	-193		
CoNC/GD	0.5 M H$_2$SO$_4$	-340@10	-138	-	[21]
	1.0 M KOH	-284@10	-115		
Mo$_2$C QD/NGCL	0.5 M H$_2$SO$_4$	-136@10	-68.4	1.0	[22]
	1.0 M KOH	-111@10	-57.8		
P-W$_2$C@NC	0.5 M H$_2$SO$_4$	-89@10	-53	3.5	[23]
	1.0 M KOH	-63@10			
1D-RuO$_2$-CN$_x$	0.5 M H$_2$SO$_4$	-93@10	-40	~0.17	[24]
	0.5 M KOH	-95@10	-70		
Zn$_{0.3}$Co$_{2.7}$S$_4$	0.5 M H$_2$SO$_4$	-80@10	-47.5	0.285	[25]
	1.0 M KOH	-85@10			
Co-C-N	0.5 M H$_2$SO$_4$	-138@10	-55	-	[26]
	1.0 M KOH	-178@10	-102		
Co-Mo-S$_x$	0.1 M HClO$_4$	~-250@5	-	0.05	[27]
	0.1 M KOH	~-201@5	-		
Mo$_2$C@2D-NPC	0.5 M H$_2$SO$_4$	-86@10	-62	0.2471	[28]
	1.0 M KOH	-45@10	-46		
NiAu/Au	0.5 M H$_2$SO$_4$	~-50@10	-36	-	[29]
RuCo@NC	1.0 M KOH	-28@10	-31		[30]

Ru@C_2N	0.5 M H_2SO_4	-13.5@10	-30	0.285	[31]
	1.0 M KOH	-17@10	-38		
Ru/C_3N_4/C	0.5 M H_2SO_4	~-75@10	-	-	[32]
	0.1 M KOH	-79@10			
C_3N_4@NG	0.5 M H_2SO_4	-240@10	-51.5	0.1	[33]
RuP_2@NPC	0.5 M H_2SO_4	-38@10	-38	1.0	[34]
Pt-Co(OH)$_2$/CC	1.0 M KOH	-32@10	-70	6.9	[35]

References

[1]   J. Tian, Q. Liu, A. M. Asiri, X. Sun, J. Am. Chem. Soc. 136 (2014) 7587–7590.

[2]   H. Tabassum, W. Guo, W. Meng, A. Mahmood, R. Zhao, Q. Wang, R. Zou, Adv. Energy Mater. 7 (2017) 1601671.

[3]   Z. Xing, Q. Liu, A. M. Asiri, X. Sun, ACS Catal. 5 (2015) 145–149.

[4]   Z. Pu, I. S. Amiinu, S. Mu, Energy Technol. 4 (2016) 1030–1034.

[5]   Z. Pu, X. Ya, I. S. Amiinu, Z. Tu, X. Liu, W. Li, S. Mu, J. Mater. Chem. A 4 (2016) 15327–15332.

[6]   W. Zhu, C. Tang, D. Liu, J. Wang, A. M. Asiri, X. Sun, J. Mater. Chem. A 4 (2016) 7169–7173.

[7]   Z. Pu, S. Wei, Z. Chen, S. Mu, Appl. Catal. B: Environ. 196 (2016) 193–198.

[8]   R. Zhang, X. Wang, S. Yu, T. Wen, X. Zhu, F. Yang, X. Sun, X. Wang, W. Hu, Adv. Mater. 29 (2017) 1605502.

[9]   Y. Tan, H. Wang, P. Liu, Y. Shen, C. Cheng, A. Hirata, T. Fujita, Z. Tang, M. Chen, Energy Environ. Sci. 9 (2016) 2257–2261.

[10]   E. J. Popczun, J. R. McKone, C. G. Read, A. J. Biacchi, A. M. Wiltrout, N. S. Lewis, R. E. Schaak, J. Am. Chem. Soc. 135 (2013) 9267–9270.

[11]   L. Feng, H. Vrubel, M. Bensimon, X. Hu, Phys. Chem. Chem. Phys. 16 (2014) 5917–5921.

[12]   P. Jiang, Q. Liu, X. Sun, Nanoscale 6 (2014) 13440–13445.

[13]   Q. Liu, J. Tian, W. Cui, P. Jiang, N. Cheng, A. M. Asiri, X. Sun, Angew. Chem. Int. Ed. 53 (2014) 6710–6714.

[14]   E. J. Popczun, C. G. Read, C. W. Roske, N. S. Lewis, R. E. Schaak, Angew. Chem. Int. Ed. 126 (2014) 5531–5534.

[15]   N. Jiang, B. You, M. Sheng, Y. Sun, Angew. Chem. Int. Ed. 54 (2015) 6251–6254.

[16]   F. Juan, J. Callejas, M. McEnaney, C. G. Read, J. C. Crompton, A. J. Biacchi, E. J. Popczun, T. R. Gordon, N. S. Lewis, R. E. Schaak, ACS Nano 8 (2014) 11101–11107.

[17]   P. Xiao, M. A. Sk, L. Thia, X. Ge, R. J. Lim, J. Y. Wang, K. H. Lim, X. Wang, Energy Environ. Sci. 7 (2014) 2624–2629.

[18]   X. Zou, X. Huang, A. Goswami, R. Silva, B. R. Sathe, E. Mikmekova, T. Asefa, Angew.

Chem. Int. Ed. 126 (2014) 4372–4376.

[19]   H. Zhang, Y. Li, G. Zhang, P. Wan, T. Xu, X. Wu, X. Sun, Electrochimi. Acta   148 (2014) 170–174.

[20]   Z. Xing, Q. Liu, W. Xing, A. M. Asiri, X. Sun, ChemSusChem 8 (2015) 1850–1855.

[21]   Y. Xue, J. Li, Z. Xue, Y. Li, H. Liu, D. Li, W. Yang, Y. Li, ACS Appl. Mater. Interfaces 8 (2016) 31083−31091.

[22]   Z. Pu, M. Wang, Z. Kou, I. S. Amiinu, S. Mu, Chem. Commun. 52 (2016) 12753–12756.

[23]   G. Yan, C. Wu, H. Tan, X. Feng, L. Yan, H. Zang, Y. Li, J. Mater. Chem. A 5 (2017) 765–772.

[24]   T. Bhowmik, M. Kundu, S. Barman, ACS Appl. Mater. Interfaces 8 (2016) 28678−28688.

[25]   Z. Huang, J. Song, K. Li, M. Tahir, Y. Wang, L. Pan, L. Wang, X. Zhang, J. Zou, J. Am. Chem. Soc. 138 (2016) 1359–1365.

[26]   S. Wang, X. Hao, Z. Jiang, X. Sun, D. Xu, J. Wang, H. Zhong, F. Meng, X. Zhang, J. Am. Chem. Soc. 137 (2015) 15070–15073.

[27]   J. S. Jirkovský, C. D. Malliakas, P. P. Lopes, N. Danilovic, S. S. Kota, K. C. Chang, B. Genorio, D. Strmcnik, V. R. Stamenkovic, M. G. Kanatzidis, N. M. Markovic, Nat. Mater. 15 (2016) 197–203.

[28]   C. Lu, D. Tranca, J. Zhang, F. R. Hernández, Y. Su, X. Zhuang, F. Zhang , G. Seifert, X. Feng, ACS Nano 11 (2017) 3933–3942.

[29]   H. Lv, Z. Xi, Z. Chen, S. Guo, Y. Yu, W. Zhu, Q. Li, X. Zhang, M. Pan, G. Lu, S. Mu, S. Sun, J. Am. Chem. Soc. 137 (2015) 5859–5862.

[30]   J. Su, Y. Yang, G. Xia, J. Chen, P. Jiang, Q. Chen, Nat. Commnu. 8 (2017) 14969.

[31]   J. Mahmood, F. Li, S. Jung, M. S.t Okyay, I. Ahmad, S. J. Kim, N. Park, H. Y. Jeong, J. B. Baek, Nat. Nanotechnol. 12 (2017) 441–446.

[32]   Y. Zheng, Y. Jiao, Y. Zhu, L. H. Li, Y. Han, Y. Chen, M. Jaroniec, S. Qiao, J. Am. Chem. Soc. 138 (2016) 16174–16181.

[33]   Y. Zheng, Y. Jiao, Y. Zhu, L. H. Li, Y. Han, Y. Chen, A. Du, M. Jaroniec, S. Z. Qiao, Nat. Commnu. 5 (2014) 3783.

[34]   Z. Pu, I. S. Amiinu, Z. Kou, W. Li, S. Mu, Angew. Chem. Int. Ed. 56 (2017) 11559–11564.

[35]   Z. Xing, C. Han, D. Wang, Q. Li, X. Yang, ACS Catal. 7 (2017) 7131−7135.